PERMEABILITY OF MUSCLE CAPILLARIES TO SMALL HEME-PEPTIDES

Evidence for the Existence of Patent Transendothelial Channels

NICOLAE SIMIONESCU, MAIA SIMIONESCU, and GEORGE E. PALADE

From the Yale University School of Medicine, New Haven, Connecticut 06510

ABSTRACT

Two heme-peptides (HP) of about 20-Å diameter (heme-undecapeptide [H11P], mol wt ~1900 and heme-octapeptide [H8P], mol wt ~1550), obtained by enzymic hydrolysis of cytochrome *c*, were used as probe molecules in muscle capillaries (rat diaphragm). They were localized *in situ* by a peroxidase reaction, enhanced by the addition of imidazole to the incubation medium. Chromatography of plasma samples showed that HPs circulate predominantly as monomers for the duration of the experiments and are bound by aldehyde fixatives to plasma proteins to the extent of ~50% (H8P) to ~95% (H11P). Both tracers cross the endothelium primarily via plasmalemmal vesicles which become progressively labeled (by reaction product) from the blood front to the tissue front of the endothelium, in three successive resolvable phases. By the end of each phase the extent of labeling reaches >90% of the corresponding vesicle population. Labeled vesicles appear as either isolated units or chains which form patent channels across the endothelium. The patency of these channels was checked by specimen tilting and graphic analysis of their images. No evidence was found for early or preferential marking of the intercellular junctions and spaces by reaction product. It is concluded that the channels are the most likely candidate for structural equivalents of the small pores of the capillary wall since they are continuous, water-filled passages, and are provided with one or more strictures of ≤100 Å. Their frequency remains to be established by future work.

According to the pore theory of capillary permeability, the wall of blood capillaries is provided with small pores which may occur as either cylinders of ~90-Å diam or slits of ~50-Å width (1–5). The structural identity and location of these pores are still in doubt. On the one hand, work carried out with HRP[1] (mol wt, 40,000; Mds ~50–60 Å [6]) and cytochrome *c* (mol wt ~12,300; Mds 30 × 34 × 34 Å [7, 8]) as probe molecules has led to the conclusion that the small pores are slits localized in the intercellular junctions of the endothelium (9–11). On the other hand, on the basis of results obtained with myoglobin (mol wt ~17,800; Mds

[1] *Abbreviations used in this paper:* HP, heme-peptide; H8P, heme-octapeptide; H11P, heme-undecapeptide; HRP, horseradish peroxidase; Mb, myoglobin; Md(s), molecular diameter(s); RP, reaction product.

23 × 35 × 43 Å [12]), we have identified the plasmalemmal vesicles of the endothelial cells as the structural equivalent of both large and small pore systems (13).

Since the tracers so far used range in size from 60 to 33 Å, they are expected to undergo considerable molecular sieving (4) while passing through ~90-Å diam channels; this evidently reduces, at least in part, their usefulness as small pore probes. Molecules smaller than 30 Å will be preferable since they would be less affected by sieving. Accordingly, we decided to use as tracers a heme-undecapeptide (H11P) (mol wt ~1900; Md ~20 Å) and a heme-octapeptide (H8P) (mol wt ~1550) which can be obtained by enzymatic digestion of cytochrome *c*. The heme-undecapeptide ("microperoxidase") was introduced as tracer by Feder (14–16), who showed that it gains access to spaces in the brain from which HRP is excluded (17).

This article presents results obtained by using H11P and H8P as probe molecules for muscle capillary permeability.

MATERIALS AND METHODS

Materials

PREPARATION OF H11P: The procedure used was basically that described by Tsou (18), Tuppy and Paléus (19), and Harbury and Loach (20) slightly modified as follows (21): 10 g of horse heart cytochrome *c*, type VI (Sigma Chemical Co., St. Louis, Mo.) dissolved in 800 ml of 0.1 N HCl, were incubated for 24 h at 24°C with 300 mg pepsin (2800 U/mg, Worthington Biochemical Corp., Freehold, N. J.). The digestion was performed at pH 1.5 and stopped by adjusting the pH to 8.5 with 2 N NaOH. The digestion product was precipitated by adding 600 g $(NH_4)_2SO_4$ and the precipitate collected by filtration under vacuum on a 1.2-μm Millipore filter (Millipore Corp., Bedford, Mass.). The red residue was washed from the filter and dissolved in 50 ml distilled water and 2 ml of 2 N NaOH. From this solution, the peptide was purified by gel filtration through a Biogel P6 column (2.5 × 90 cm) equilibrated with 0.1 M NH_4HCO_3 at pH 8.0. The effluent, bearing the main fraction at the expected position of a ~1800–2000 mol wt peptide, was collected separately and lyophilized *in vacuo* at −50°C. The powder pooled from several runs was dissolved in 20 ml distilled water and 1.5 ml of 2 N NaOH and rechromatographed for further purification.

PREPARATION OF H8P: The preparation of H8P was carried out according to the procedure of Harbury and Loach (20) as modified by Kraehenbuhl et al. (21): 100 mg of H11P were dissolved in 20 ml of 0.1 M NH_4HCO_3, pH 8.0, and the solution was incubated with 10 mg trypsin (two times crystallized, Worthington Biochemical Corp.) for 36 h at 37°C. At 12-h intervals, fresh trypsin was added in concentration equivalent to 5% of the weight of the heme-peptide. The digestion product was lyophilized, disolved in 5 ml distilled water, and passed through the Biogel P6 column mentioned above. The main red peak was collected, lyophilized, and rechromatographed until a symmetrical peak was obtained. Further purification was achieved by countercurrent distribution in butanol, pyridin, 0.1% acetic acid by 2,000 transfers.[2]

Fig. 1 shows the primary structure of these two HPs and the levels at which the polypeptide chains of cytochrome *c* and H11P are split by pepsin and trypsin, respectively.

Comparative data concerning some physical and chemical characteristics of cytochrome *c*, H11P, and H8P are presented in Table I. Fig. 1 and Table I are based on data taken from the literature (15, 16, 20).

PREPARATION OF TRACER SOLUTIONS: H11P or H8P powder was dissolved in 0.154 M NaCl at concentration of 0.5% (wt/vol) and the pH of the solution was adjusted to 7.0 with 0.1 N NaOH.

ANIMALS: We used rats of the Wistar-Furth strain (Microbiological Associates, Inc., Bethesda, Md.) known to be genetically resistant to histamine release by a variety of agents (22–24); control experiments showed that HPs topically applied (0.25 mg in 50 μl) in a cremaster test (25) do not cause vascular leakage in this strain. We used 89 male, young adult animals (110–130 g) for tracer experiments and 59 for different controls (Table II). Before the experiments, all animals were kept for 3 days under standardized housing and feeding conditions.

Methods

DETERMINATION OF HP STATE IN TRACER SOLUTIONS AND BLOOD PLASMA: Gel filtration (Biogel P6 column 2.5 × 90 cm, with 0.1 M NH_4HCO_3 as eluant), followed by absorbtiometry (at 280 nm) and by spectrophotometry (at 417 nm for H11P and 410 nm for H8P) of the eluate, was used to check the purity, size, and and dispersion of H11P and H8P in (*a*) tracer solutions, (*b*) tracer solutions treated for 2 h at 24°C with aldehydes, (*c*) plasma or serum collected 10 min after tracer injection, and (*d*) plasma samples collected as above and treated for 2 h at 24° with the aldehyde mixture used for tissue fixation.

TRACER INJECTIONS: HPs solutions were injected intravenously following the procedure given in (13) and using a lower concentration (0.5% wt/vol) than previous workers (14, 17). The tracer solutions (1 ml/100 g body weight) were well tolerated by the animals.

OSMOMETRY: The osmolality of the plasma was monitored at successive time intervals after injection of the tracer in the femoral vein. Blood samples (1 ml),

[2] Dr. J. P. Kraehenbuhl kindly prepared for us the highly purified H8P used in most of these experiments.

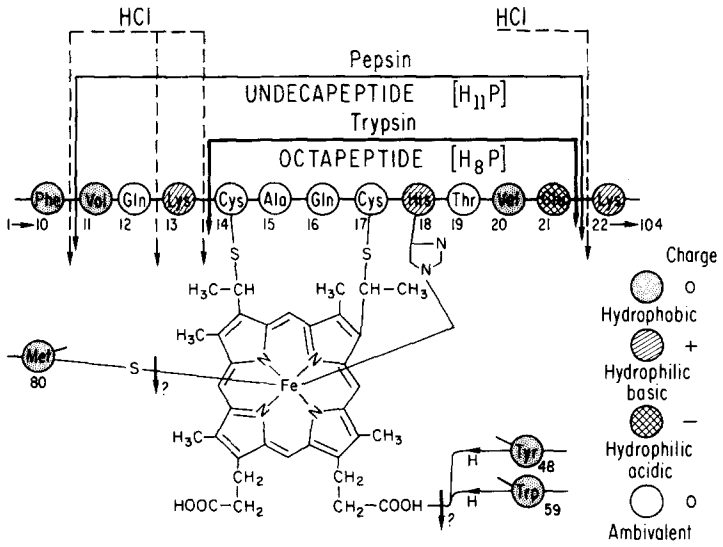

Abbreviations used in legends:

bm, basement membrane
c, transendothelial channels
cf, collagen fibers
e, endothelium
i, infundibulum
is, intercellular space (endothelium)
j, intercellular junction
l, capillary lumen
m, muscle cell
n, nucleus
p, pericyte
pp, pericyte pseudopodium
pv, plasmalemmal vesicle in pericytes
rbc, red blood cell
s, stricture
sv, sarcolemmal vesicle
v, plasmalemmal vesicle
vb, plasmalemmal vesicle (blood front)
vi, plasmalemmal vesicle (inside the cytoplasm)
vt, plasmalemmal vesicle (tissue front)

FIGURE 1 The diagram shows the sites at which the polypeptide chain of the cytochrome *c* molecule is split by successive treatment with HCl, pepsin, and trypsin. In both H11P and H8P the heme is covalently bound to the peptide chain by thio-ether bridges to the cysteinyl residues 14 and 17 and by a coordination bound between the Fe atom and the imidazole nitrogen of His 18 (7, 8). The bond of Fe to Met 80 as well as the hydrogen bonds to Tyr 48 and Trp 59 are broken. The conformation of these HP molecules is still unknown. Two basic residues in the undecapeptide chain versus one in the octapeptide chain introduce a difference in their pH optimum (20, 27) which was taken into consideration in setting up the incubation media for the peroxidatic reaction (see Methods).

collected from the aorta on heparin (15 U of heparin in 0.2 ml isotonic saline), were spun in a microfuge (model 152, Beckman Instruments, Inc. Spinco, Div., Palo Alto, Calif.) at 10,000 rpm for 2 min and the supernate was assayed in a Fiske OFTM osmometer (Model 330 D-Fiske Associates, Inc., Uxbridge, Mass.).

TISSUE FIXATION: Fixation of the diaphragm, carried out *in situ* as in reference 13, was started either simultaneously with the HP injection, or at chosen intervals from 1 s to 15 min after it (Table II). On the basis of results obtained in our Mb experiments (13), we assumed that the hemolysis induced by fixation was negligible, and the time required for the arrest of the local blood flow by the fixative amounted to ~25 s; hence, all time points were corrected for this figure.

CYTOCHEMICAL PROCEDURE: For the demonstration of the peroxidatic activity of HPs (21), we applied the Graham-Karnovsky method (26) as modified in our Mb experiments (13). In addition, the incubation medium was supplemented with 0.1 M imidazole, since it is known that this nitrogenous ligand increases significantly the peroxidatic activity of both H11P and H8P (27). The imidazole effect made possible a substantial reduction in the amount of tracer injected. The final composition of the incubation medium was: 0.15% 3,3'-diaminobenzidine tetrahydrochloride, 0.02% H_2O_2 and 0.1 M imidazole in 0.05 M Tris-HCl buffer, at pH 8.6–9.0 for H11P and 7.0–7.2 for H8P. The reaction was carried out at room temperature for 60 min, and the tissue was subsequently processed as in reference 13. Before dehydration, a number of specimens were treated in block with a 1% solution of digallic acid[3]; this treatment gives

[3] Simionescu, N., and M. Simionescu. 1975. Digallic acid as mordant for electron microscope specimens. Manuscript in preparation.

TABLE I

*Comparative Data on Cytochrome c and Derived Hemepeptides**

	Cytochrome *c*	H11P	H8P
Number of amino acids	104	11	8
Side chains			
Hydrophobic	33	2	1
Hydrophilic, basic‡	24	2	1
Hydrophilic, acidic	7	1	1
Ambivalent§	29	6	5
Glycine	11	0	0
mol wt	12,384	1,900	1,550
Mds.	30 × 34 × 34	~20	≲ 20
Peroxidatic activity‖	0.019	1.9	2.9
In the presence of imidazole	0.018	3.4	7.4
Optimal pH	6.0	9.2	7.0

* Data taken from references (7, 8, 16, 18–20, 28–40)

‡ Located on the surface of the molecule, they are the main groups involved in interaction with other molecules including aldehydes during fixation.

§ Small hydrophobic, or uncharged polar residues.

‖ *o*-dianisidine units (27).

TABLE II

*Time Intervals and Number of Animals Used**

Tracer	Intervals‡ 0–30 s phase I	30–40 s phase II	40–60 s phase III	1–3 min	5–15 min	Total number of animals
H11P	11	14	15	6	4	50
H8P	10	9	12	4	4	39
Controls						59

* For each rat, four to seven samples of diaphragm were examined by electron microscopy.

‡ Intervals counted from the beginning of the i.v. injection of the tracer and corrected for the time needed to arrest the blood flow by fixation *in situ* (average: 25 s) (see Methods).

an enhanced contrast of the plasmalemma and vesicular membranes of the endothelium.

Controls for possible diffusion of HPs or their reaction product (RP) into the tissue (26) were carried out by adding HPs to the fixative solution or to the incubation medium (13).

RESULTS

State of Heme-Peptides

IN THE TRACER SOLUTIONS: Gel chromatography followed by spectrophotometry of the eluate showed that (Fig. 2) (*a*) H8P elutes as a single, symmetrical peak at the expected position of the monomer; and (*b*) H11P also elutes at the expected position of its monomer, but as a slightly asymmetrical peak preceded by a shoulder and followed by a tail, which indicated that the preparation contains some aggregates (~5% of total) and a few contaminants of small molecular weight.

IN THE CIRCULATING BLOOD: Gel chromatography of plasma samples collected 10 min after HP injection showed that (Fig. 3) (*a*) H8P retains its monomeric dispersion and binds to the extent of maximum 12% to plasma proteins; (*b*) 2-h treatment of a similar sample with aldehyde fixative results in about 50% binding of this peptide to plasma proteins; (*c*) H11P behaved slightly less favorably than H8P in the circulating plasma:

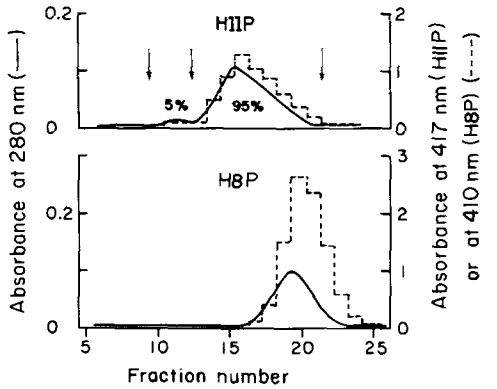

FIGURE 2 Elution profiles of H11P and H8P solutions (0.5% wt/vol) in 0.15 M NaCl, pH 7.0. Biogel P6 column (2.5 × 90 cm) equilibrated and eluted with 0.1 M NH_4HCO_3, pH 8.0, at 4°C and 20 ml/h.

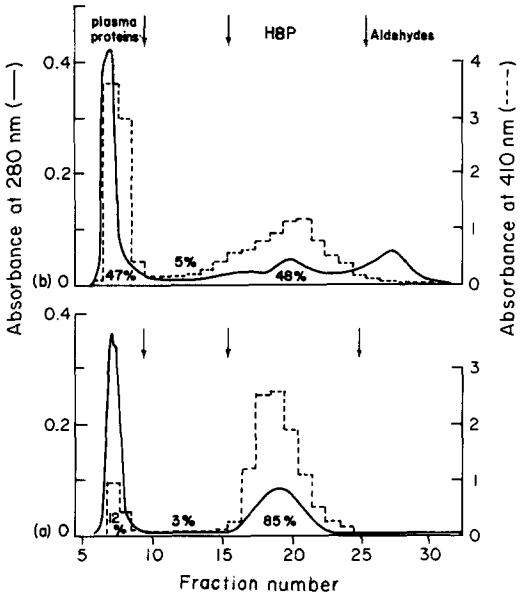

FIGURE 3 Gel chromatography (Biogel P6) of a plasma sample (0.25 ml) collected 10 min after i.v. injection of 1 ml/100 g body weight of 0.5% H8P solution in a rat with ligated renal vessels. Absorbance at 280 nm: —; absorbance at 410 nm: - - -. (*a*) untreated plasma sample, (*b*) plasma sample treated with aldehydes (see Methods) for 2 h at 24°C. Absorbance at 410 nm is due to monomeric H8P in fractions 15–25; mostly hemoglobin (cf. 13) in fractions 6–9 in Fig. 3 *a* and mostly H8P bound to plasma proteins in the same fractions in Fig. 3 *b*. Figures give percentage of absorbance at 410 nm for the fractions indicated by vertical arrows.

the peak is broader and ~16% of the tracer is bound to plasma proteins; (*d*) aldehydes, however, bind this peptide almost quantitatively to plasma proteins (Fig. 4).[4]

Similar results were obtained when serum instead of plasma was assayed and when in vitro mixtures of plasma (or serum) and HP were used.

These findings indicate that the HPs remain in predominantly monomeric form in both tracer solution and circulating blood over the period relevant for our observations. H8P is more uniformly dispersed, but H11P is more efficiently retained by fixation.

[4] Control experiments showed that a 2-h treatment of the tracer solutions with aldehyde fixative (in conditions similar to those indicated in Figs. 3 and 4) led to the formation of aggregates of polymers (30% of total) of lower molecular weight than HPs cross-linked to plasma proteins. Such aggregates are not detected in samples of plasma fixed after the injection of the tracer.

Changes in Plasma Osmolality after HP Injection

The osmolality of the plasma determined in a group of 10 control animals gave a mean of 325 ± 8 (SD) mosmol/kg H_2O (SD between duplicate samples was ± 4).

The measured osmolality of the injected solution (0.5% wt/vol H11P in 154 mM NaCl) was 309 ± 2, a figure which comes very close to the theoretically expected value of 310.63.

In vitro mixtures of plasma and tracer solution (0.3 ml plasma + 0.06 ml of 0.5% wt/vol H11P in 154 mM NaCl) showed an expected slight decrease (~1.8%) in osmolality.

Samples collected from the aorta of 21 animals, at 15, 30, and 45 s, after intravenous (i.v.) tracer injection, showed however, a slight increase

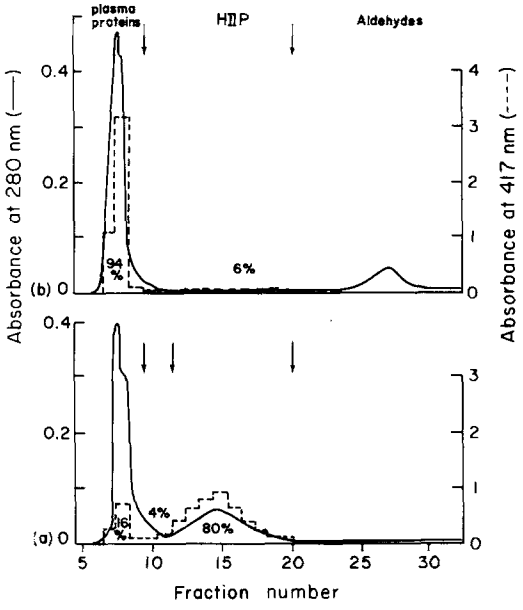

FIGURE 4 *a,b* Gel chromatography (Biogel P6) of a plasma sample (0.25 ml) collected 10 min after injecting intravenously 1 ml/100 g body weight of 0.5% H11P solution in a rat with ligated renal vessels. Absorbance at 280 nm: —; absorbance at 417 nm: - - -. (*a*) Untreated plasma sample, (*b*) plasma sample treated with aldehydes (see Methods) for 2 h at 24°C. In *a*, the material absorbing at 417 nm is monomeric H11P in fractions 12–20, probably polymers or aggregates of H11P in fractions 9–11, and H11P bound to plasma proteins in addition to hemoglobin (cf. 13) in fractions 6–8. In *b*, the small amount of material absorbing at 417 nm in fractions 9–25 is probably unbound H11P, while the large amount in fractions 6–9 is H11P bound to plasma proteins. Figures give percentage of total absorbance at 417 nm for the fractions indicated by vertical arrows.

(~1.2%) of plasma osmolality (329 ± 12 mosmol/kg H_2O at 15 sec, 328 ± 11 mosmol/kg H_2O at 30 s, and 329 ± 7 mosmol/kg H_2O at 45 s) for which we do not have at present an explanation. At least 6 animals were used for each time point.

Diffusion of HPs and their RP into the Tissue

Under our experimental conditions, there was no evidence of HP diffusion from the fixative solution into either interstitia or cells along the cut surfaces of the tissue blocks. The same applies for the diffusion of HPs or their RP from the incubation medium into the tissue.

HPs Pathway Across the Capillary Wall

To insure adequate sampling, specimens from 9 different animals were examined for each early time point (up to 60 s). For each specimen, 30–45 capillary profiles were micrographed and used for collecting the data. The aggregate endothelial volume examined amounted to 15.6 μm^3 and comprised a total population of ~10,400 vesicles (Table III).

At each time point, the pattern of vesicular labeling observed showed a certain degree of variation from one capillary to another, but there was a recognizable predominant pattern for each of the intervals considered (Table IV).

CAPILLARY LUMEN: Up to 60 s, RP was generally abundant, compact, and evenly distributed throughout the plasma. After 1–3 min the intensity of the reaction began to decrease noticeably.

ENDOTHELIUM: Within the endothelium, RP was detected only in plasmalemmal vesicles. The kinetics of vesicular labeling suggest that three phases of unequal duration can be distinguished during the HP passage across the most active parts of the endothelial cell, i.e. the peripheral zone and the perinuclear cytoplasm (13). The earliest detectable phase (specimens fixed from 0 to 5 s post tracer injection) was characterized by the labeling of practically all plasmalemmal vesicles on the blood front, ~20% of those located in the interior of the endothelium and none of those associated with the tissue front (Table V). Since arrest of the blood flow by the fixative requires ~25 s, the micrographs of these specimens (Figs. 5 and 8) demonstrate the situation in the endothelium 25–30 s after injection. This condition which was designated *phase I* (till 30 s) corresponds to phases I and II in our Mb experiments (13). HPs appear to penetrate the vesicular system more rapidly than Mb. By the end of this phase, approximately 40% of the total vesicle population was labeled (Figs. 5, 8). The reaction product was found in the infundibula leading to the junctions, but was not detected in the intercellular spaces beyond the junctions (Fig. 11 *a*).

PHASE II (30–40 s): Vesicular labeling within the blood front group remained as extensive as in phase I, while in the inner group it reached ~70%; in addition, labeled vesicles began to appear on the tissue front (Figs. 6 and 9). The extent of labeling within the total vesicle population exceeded 50%. The situation of the junctions remained as described for phase I.

PHASE III (40–60 s): Vesicular labeling increased to ~90% in the inner group and in that on the tissue front. On the latter, more than 60% of the vesicles were open, apparently discharging their content in the pericapillary spaces. In such vesicles, the RP density was often higher than in the adjacent interstitia (Figs. 7 and 10). About 93%

TABLE III

Aggregate Volume of Endothelium and Number of Vesicles Examined

	H11P				H8P			
	Rest of cytoplasm*		Perinuclear cytoplasm		Rest of cytoplasm*		Perinuclear cytoplasm	
Time intervals	Aggregate volume	No. of vesicles	Aggregate volume	No. of vesicles	Aggregate volume	No. of vesicles	Aggregate volume	No. of vesicles
	μm^3		μm^3		μm^3		μm^3	
0–30 s (phase I)	1.81	1,109	1.44	1,011	1.32	938	1.04	715
30–40 s (phase II)	1.64	942	1.27	815	1.20	747	1.13	744
40–60 s (phase III)	0.92	590	1.26	869	1.41	979	1.22	854
Total	4.37	2,641	3.97	2,695	3.93	2,664	3.39	2,313

* Mainly peripheral zone with minor contributions from the parajunctional zone and the organelle region.

TABLE IV

Percentage of Capillary Profiles Showing Different Patterns of Vesicular Labeling as a Function of Time

Time intervals*	Vesicular labeling: Blood front and inside	Blood front, inside, and tissue front	All positions and labeling of the pericapillary space
	(Range)	(Range)	(Range)
0–30 s phase I	91 (75–100)	9 (0–25)	0
30–40 s phase II	79 (68–88)	20 (12–29)	1 (0–3)
40–60 s phase III	1 (0–5)	8 (0–35)	91 (60–100)

* For each interval an average number of 100 capillary profiles were examined.

of the total vesicle population was marked in each of the two main regions of the endothelium, the peripheral zone and the perinuclear cytoplasm. At this time period, the most striking feature was the existence of chains of vesicles, some of them forming apparently continuous channels across the endothelium. They will be described in more detail in a separate section. During phase III, while the infundibula leading to the junctions were marked by RP of *density* equal to that found in the lumen, the intercellular spaces beyond the junctions contained RP in concentrations lower or equal to that found in the pericapillary spaces. In some cases, the dense RP of the lumen appeared clearly limited at the level of a tight junction (Fig. 11 *b*).

In phase III, the labeling of the pericapillary spaces by RP was rapid and general; it also appeared to be quasi-uniform so that concentration gradients of the type encountered in experiments with larger tracers (11, 13) were not de-

TABLE V

*Percentage of Marked Vesicles in the Three Groups of Plasmalemmal Vesicles at Different Time Intervals after Tracer Injection**

Time intervals	H11P Experiments: marked plasmalemmal vesicles %: Total	Blood front	Inside	Tissue front	H8P Experiments: marked plasmalemmal vesicles %: Total	Blood front	Inside	Tissue front
0–30 s phase I	38 ± 8	80 ± 14	35 ± 11	0	39 ± 9	86 ± 9	31 ± 10	0
30–40 s phase II	58 ± 10	91 ± 6	68 ± 15	15 ± 8	57 ± 10	88 ± 8	62 ± 19	21 ± 4
40–60 s phase III	93 ± 6	95 ± 4	89 ± 7	94 ± 6	95 ± 5	97 ± 3	91 ± 6	96 ± 4

For each phase, a number of 520–610 vesicles were counted for H11P and 560–640 for H8P experiments. As in our previous study (58), the distribution of vesicles was as follows: ~30% on the blood front, ~30% in the interior of the cytoplasm, and ~40% on the tissue front of the endothelium.

* The data refer only to the peripheral zone of the endothelial cells.

FIGURE 5 Rat diaphragm. Blood capillary 30 s after an H8P injection (phase I). The RP marks the capillary lumen (*l*), all plasmalemmal vesicles open on the blood front of the endothelium (*vb*), and some of those located within the endothelial cytoplasm (*vi*). The vesicles associated with the tissue front (*vt*) and the pericapillary spaces (*ps*) are free of RP. × 60,000.

FIGURE 6 Rat diaphragm. Blood capillary 35 s after H8P injection (phase II). Concomitantly with the vesicles open on the blood front (*vb*), the RP marks a high percentage of vesicles located within the endothelial cytoplasm (*vi*). A number of vesicles are labeled on the tissue front (*vt*), but there is no evidence of tracer discharge into the pericapillary space (*ps*). Sarcolemmal vesicles (*sv*) are still unmarked. × 42,000.

FIGURE 7 Rat diaphragm. Blood capillary 60 s after H8P injection (phase III). Extensive labeling of plasmalemmal vesicles on the blood front (*vb*), inside the cytoplasm (*vi*), and on the tissue front (*vt*) has been attained. Note two apparent channels formed by chains of vesicles (c_1 and c_2) connecting the two endothelial fronts. Specimen tilting resolved the connection at *r* into overlapping, separate vesicles, while the channel c_1 retained its continuity. × 60,000.

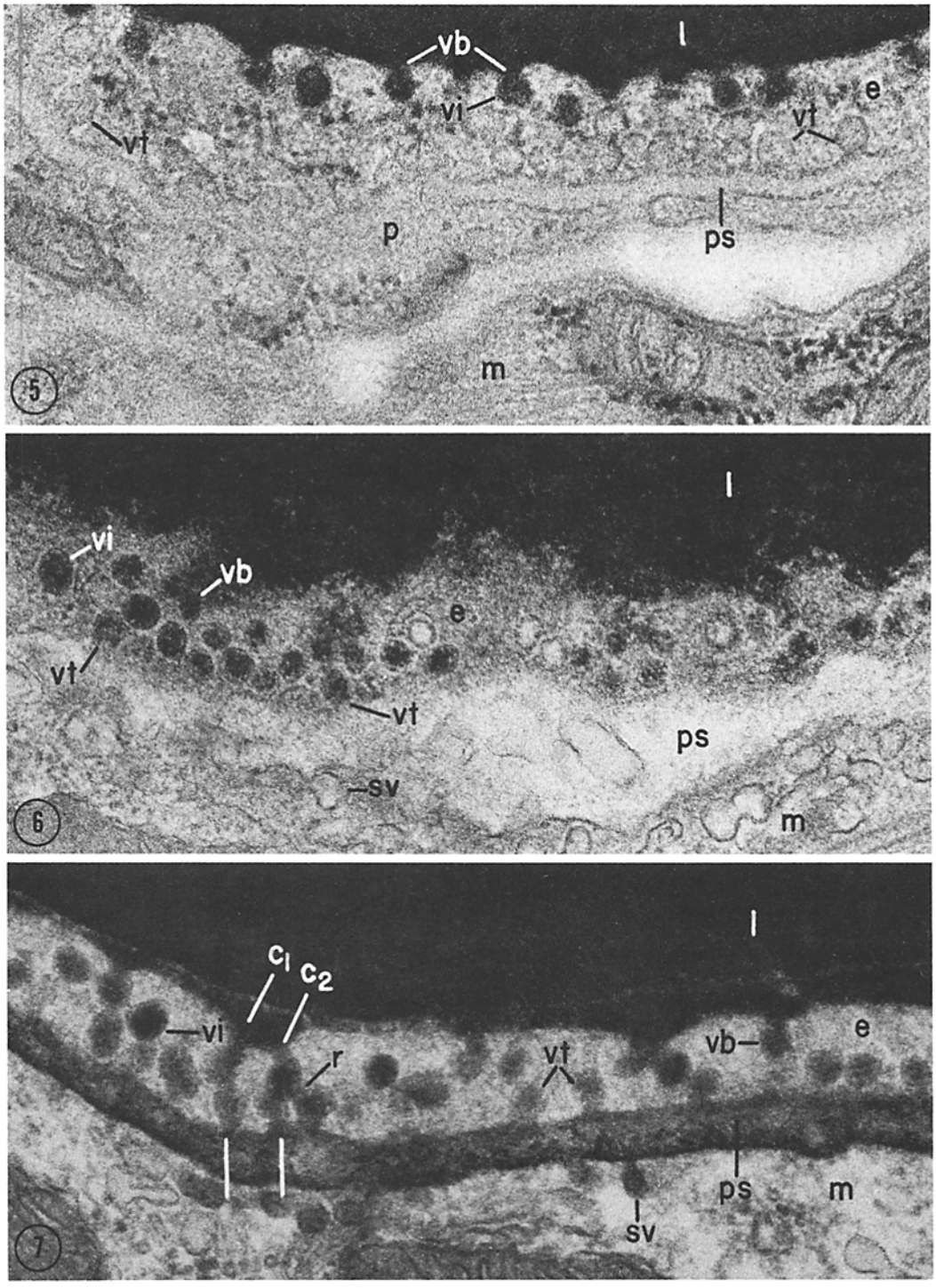
vb
l
vi
e
vt
vt
p
ps
m
5
l
vi
vb
e
vt
vt
ps
sv
m
6
l
c1
c2
vi
r
vt
vb
e
ps
m
sv
7

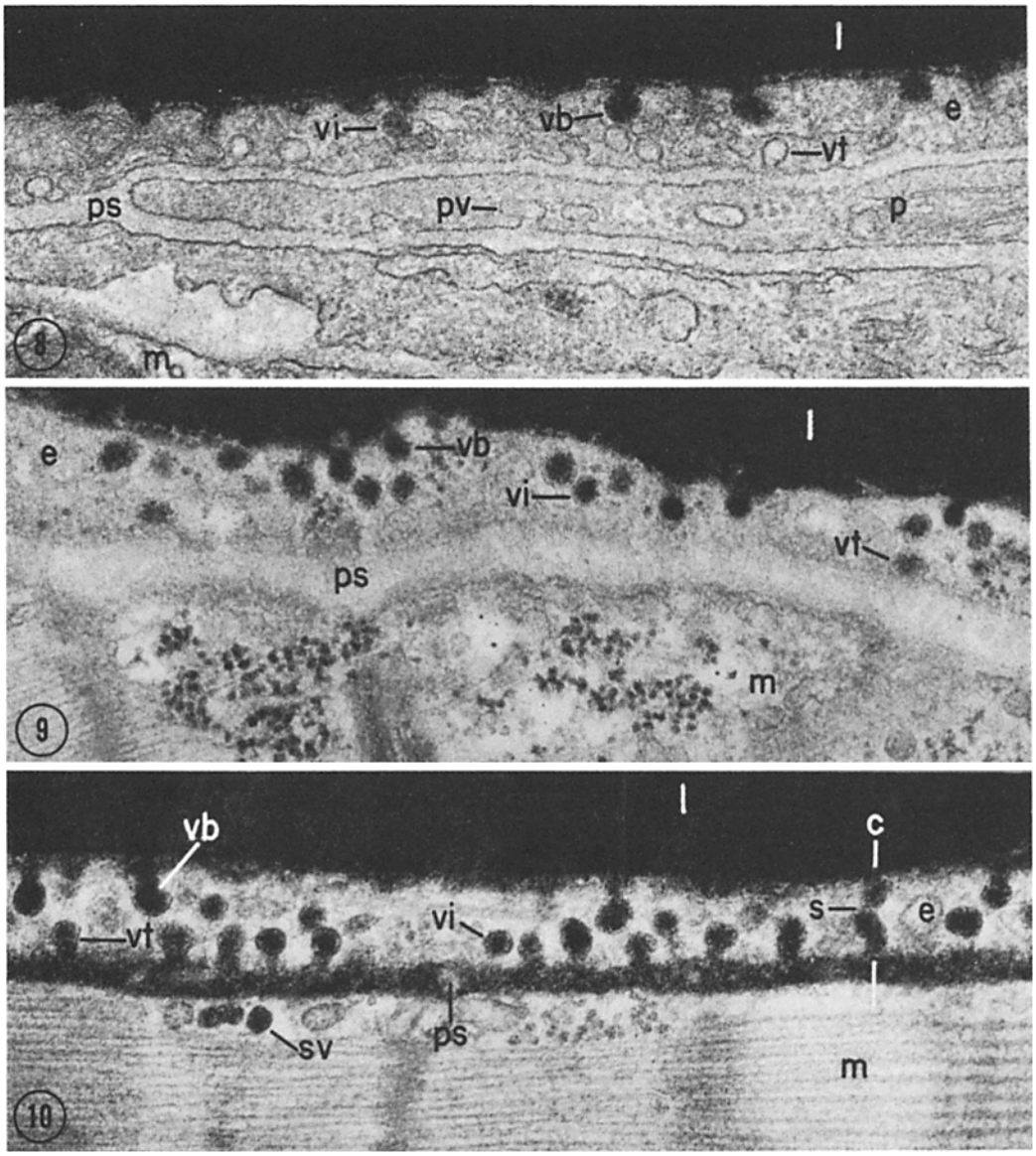

FIGURE 8 Rat diaphragm. Blood capillary 30 s after H11P injection (phase I). RP is present in the capillary lumen (*l*) and in all plasmalemmal vesicles open on the blood front (*vb*). Few of the vesicles located inside the cytoplasm (*vi*) are also labeled. The vesicles associated with the tissue front (*vt*), the pericapillary spaces (*ps*), the plasmalemmal vesicles of pericytes (*pv*), and the sarcolemmal vesicles are unlabeled. × 42,000.

FIGURE 9 Rat diaphragm. Blood capillary 35 s after H11P injection (phase II). In addition to the labeling of all vesicles on the blood front (*vb*) and most of those located inside the endothelial cytoplasm (*vi*), two vesicles associated with the tissue front (*vt*) are marked by RP in high concentration. The pericapillary spaces (*ps*) are still free of label. × 35,000.

FIGURE 10 Rat diaphragm. Blood capillary 60 s after H11P injection (phase III). Almost all plasmalemmal vesicles in all three locations are labeled. Note the chain of two vesicles at *c*. × 40,000.

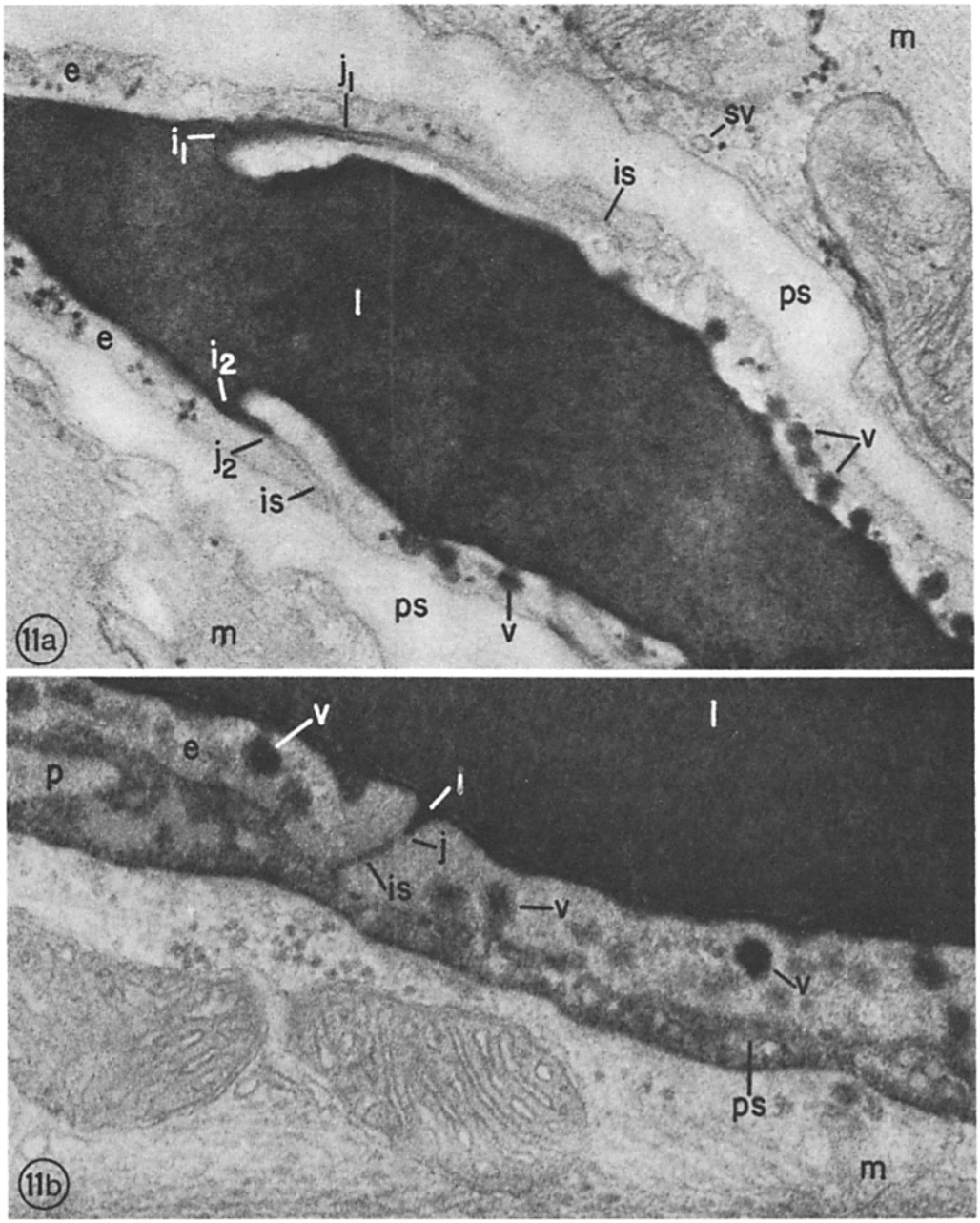

FIGURE 11 *a,b* Rat diaphragm. Blood capillary: intercellular junctions of the endothelium at different intervals after H8P i.v. administration. (*a*) 35 s post tracer injection (phase I) the RP marks the infundibula (i_1 and i_2) leading to the junctions (j_1 and j_2). The intercellular spaces (*is*) beyond the junctions are free of RP. (*b*) 60 s after tracer injection (phase III), at the time when most plasmalemmal vesicles (*v*) are labeled (including those opened on the tissue front), RP is present within the infundibulum (*i*) in the same concentration as in the capillary lumen (*l*), but shows a sharp stop at the level of the tight junction (*j*). The intercellular spaces (*is*) beyond this junction contain RP in concentration equal to that found in the adjacent pericapillary space (*ps*). a, × 35,000; b, × 48,000.

tected. The situation probably reflects the rapid diffusion of HPs in the tissue spaces.[5]

Past 3 min, the capillary lumen, the plasmalemmal vesicles, the intercellular spaces of the endothelium, and the pericapillary spaces were uniformly marked by RP of noticeably lower density than found at earlier time intervals.

In the organelle region and parajunctional zone, the pattern of vesicular labeling followed a course similar to that described in our Mb experiments (13).

BASEMENT MEMBRANE AND PERICAPILLARY SPACES: From the beginning of phase III, RP uniformly filled all spaces beyond the endothelium with the exception of those occupied by collagen fibers. Basement membranes did not appear in negative contrast, suggesting that they retained the HPs partially and transiently or had a high affinity for their RP. In some specimens, RP in higher concentration than in the pericapillary spaces was observed in the plasmalemmal vesicles of pericytes and muscle fibers (Figs. 7 and 10).

Patent Channels across the Endothelium

The most interesting finding in these experiments concerned the existence of vesicle-derived transendothelial channels. These channels, located in the peripheral zone of the endothelial cell, were formed by two or more fused vesicles (occasionally by a single one) and appeared to be provided with strictures of ~100 Å (range 80–150 Å), either at their openings or at fusion sites between individual vesicles (Figs. 12–14). Channels were encountered in practically all specimens in phase III, irrespective of the HP used as tracer.

Since such appearances could represent overlapping images of vesicles otherwise isolated in the depth of the sections, 22 apparent channels were selected for further examination in an electron microscope (Siemens Elmiskop 101) provided with a stage tiltable from +23° to −23° in two perpendicular directions. The apparent channels were selected on the basis of the following criteria: (*a*) section thickness no greater than ~700 Å; (*b*) endothelium thickness no greater than ~1500 Å; (*c*) channel image compatible with an overlap no larger than ~200 Å. These limits were imposed to make sure (see below) that an overlap, if present, could be resolved with the degree of tilting available. Given the known diameter of vesicles and the endothelium thickness in the selected specimens, an overlap of open vesicles would be possible only if the vesicles were located at different levels in the depth of the section. Fig. 17 shows a graphic reconstruction of an actual image in which the vesicular profiles measured 600 Å and 650 Å in diameter. The section is assumed to be 700 Å thick. The image is analyzed for the overlap alternative (as opposed to true channel). In this case, a tilting of 23° would be sufficient to resolve an overlap of 100 Å by revealing a clear space of 180 Å between the two vesicles. Four apparent channels were resolved into overlapping but otherwise isolated vesicles (Fig. 15); 18 channels remained apparently continuous over the entire angle of tilt (Fig. 16). If the assumed section thickness were reduced to 600 Å, the resolved interval would become 100–110 Å for an overlap of 100 Å. If the overlap were increased to ~200 Å, a 23° tilt would still be sufficient to resolve a space of ~80 Å between overlapping vesicles. The tilting range used (46° = +23° to −23°) should also resolve overlap in thinner sections down to ~ 400–500 Å, which is practically the limit within which two half vesicles can be accommodated. A graphic analysis of the type illustrated in Fig. 17 was carried out for each of the remaining 18 channels. Since no clear spaces between vesicles were detected, we consider that these images represent true channels.

In specimens processed for the demonstration of peroxidatic activity, membranes in general are poorly defined. Since we felt that the demonstration of continuous channels would be considerably facilitated by adequate membrane staining, we recently worked out a procedure based on the use of digallic acid as mordant to increase membrane contrast[3]. The specimens used were taken from either control- or HP-injected animals. Fig. 18 shows that with this procedure it is possible to detect continuity between the plasmalemma and the vesicle membranes at both openings of the channels. To obviate the necessity of tilting, most of the images selected for Fig. 18 illustrate channels formed by a single vesicle. In this case tilting is not necessary if membrane continuity is detected at both openings of the channel.

[5] A rough estimate of the diffusion coefficient of H11P (calculated as in reference 13) gave figures ranging from 7.4×10^{-4} cm/s to 7.4×10^{-3} cm/s (depending on the assumed viscosity of the interstitial fluid). Given these limits, the HP molecule is expected to move in the interstitial matrix at an approximate rate of 7.4–74 μm/min.

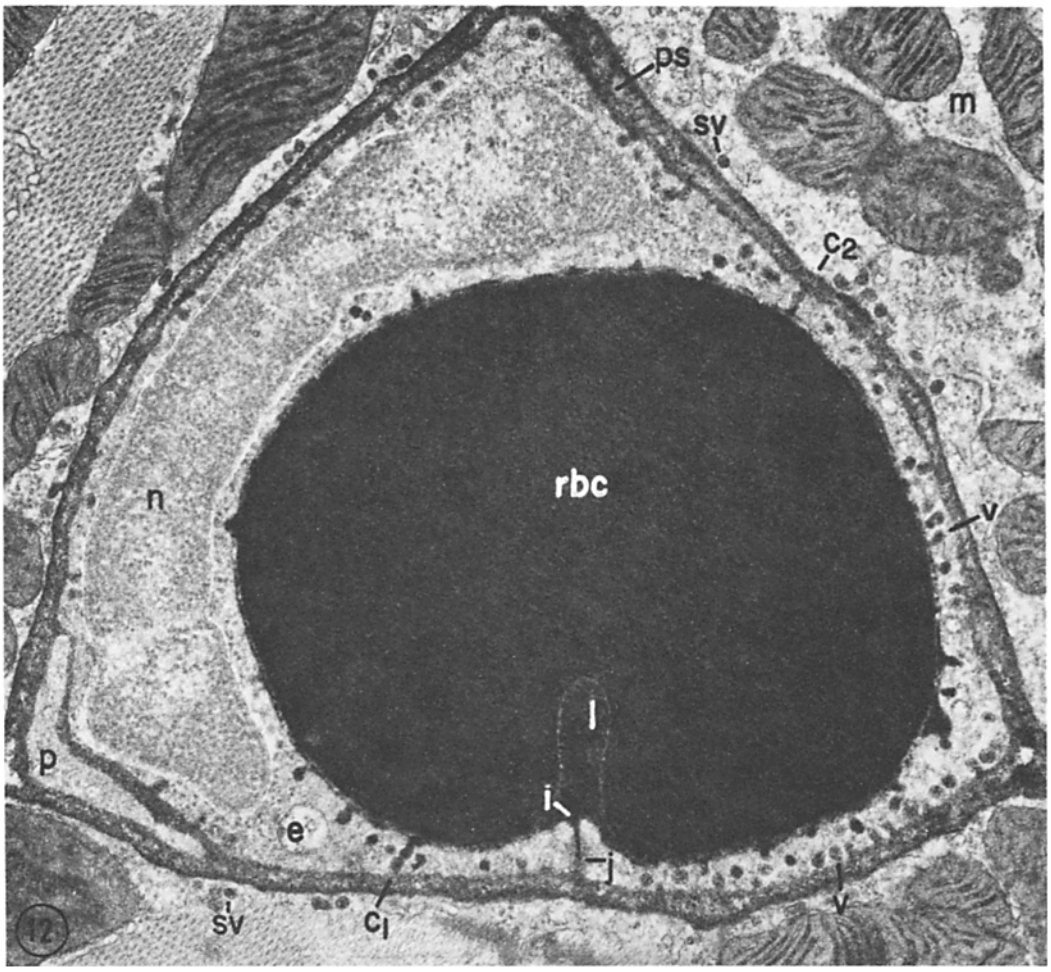

FIGURE 12 Rat diaphragm. Blood capillary 2 min after H8P injection. RP marks the capillary lumen (*l*), plasmalemmal vesicles in all positions (*v*), two transendothelial channels (c_1 and c_2), and the infundibulum (*i*) leading to the junction (*j*). Beyond the junction and in the pericapillary spaces (*ps*), RP concentration is lower than in the lumenal plasma. × 18,000.

DISCUSSION

H11P and H8P as Probe Molecules

DIMENSIONS: Myoglobin, the mass tracer used in our previous studies (13), has a mol wt of 17,800 and well established molecular dimensions (25 × 34 × 42 Å). H11P and H8P, the tracers used in the experiments now reported, are much smaller: ~1,900 and 1,550 mol wt, respectively; their dimensions are expected to be commensurately smaller, but have not been determined directly. The calculated 17–20-Å diameter given by Feder for H11P (16) is probably a maximal value since it is predicated on the assumption that the molecule is spherical.[6] The dimensions of H8P should be only slightly smaller. With a diameter of $\lesssim$20 Å, the two HPs are adequate probes for the small pore system and are expected to be less affected by molecular sieving than HRP or Mb. In

[6] This is a rough estimate based on the assumption that the molecule is spherical and that its diameter equals the cube root of the molecular weight (~1,900) (16). The estimate may be close enough to the true dimensions of H11P molecule since by X-ray analysis the diameter of the "heme-core" is ~10 Å (16). The dimensions of the cytochrome *c* molecule, disregarding the exterior side chains, are ~25 × 25 × 37 Å (34), while those of ferricytochrome *c* including the side chains are ~30 × 34 × 34 Å (8).

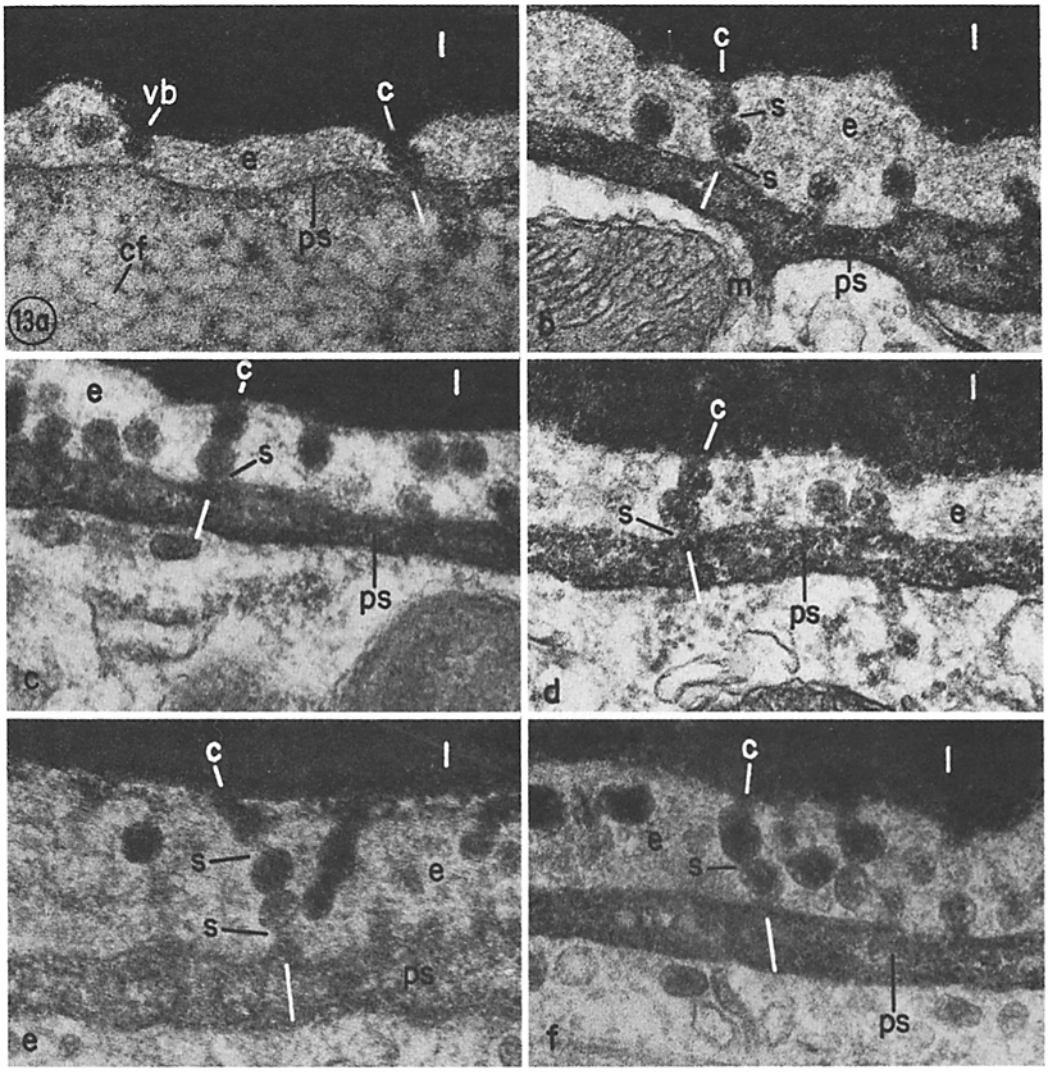

FIGURE 13 *a–f* Rat diaphragm. Blood capillaries 1–2 min after H11P injection. The figures illustrate a series of channels consisting of either a single vesicle (13 *a*) or a chain of two (13 *b*, *c*, *d*) or three vesicles (13 *e*, *f*). Note the variation in the general morphology of the channels and the existence of strictures at the connecting points or at the opening of the channels on either the blood or tissue front. A white line marks the opening of the channels on the tissue front. × 60,000.

fact, they are the smallest probes so far used for this type of work. Naturally, the HPs will permeate also the large pore system.

PEROXIDATIC ACTIVITY: The peroxidatic activity of both HPs is about 100 to 200 times stronger (27) than that of the cytochrome *c* from which they are prepared and is enhanced two to three times by imidazole (27). On the basis of available data, it can be assumed that the relatively high peroxidatic activity of HPs is due to the exposed position of their heme: both electron transfer sites (the iron and periphery of the porphyrin ring) are accessible to substrate and acceptor in the redox reactions (8, 32–36, 41). The imidazole effect could be explained by the formation of a third electron transfer site in an porphyrin-iron-imidazole coordinate (20, 30, 37, 38, 42, 43).

Experimental Conditions

OSMOLALITY CHANGES: On account of their relatively high peroxidatic activity and of the imidazole effect, we were able to use HPs at relatively small concentrations (5 mg/100 g body

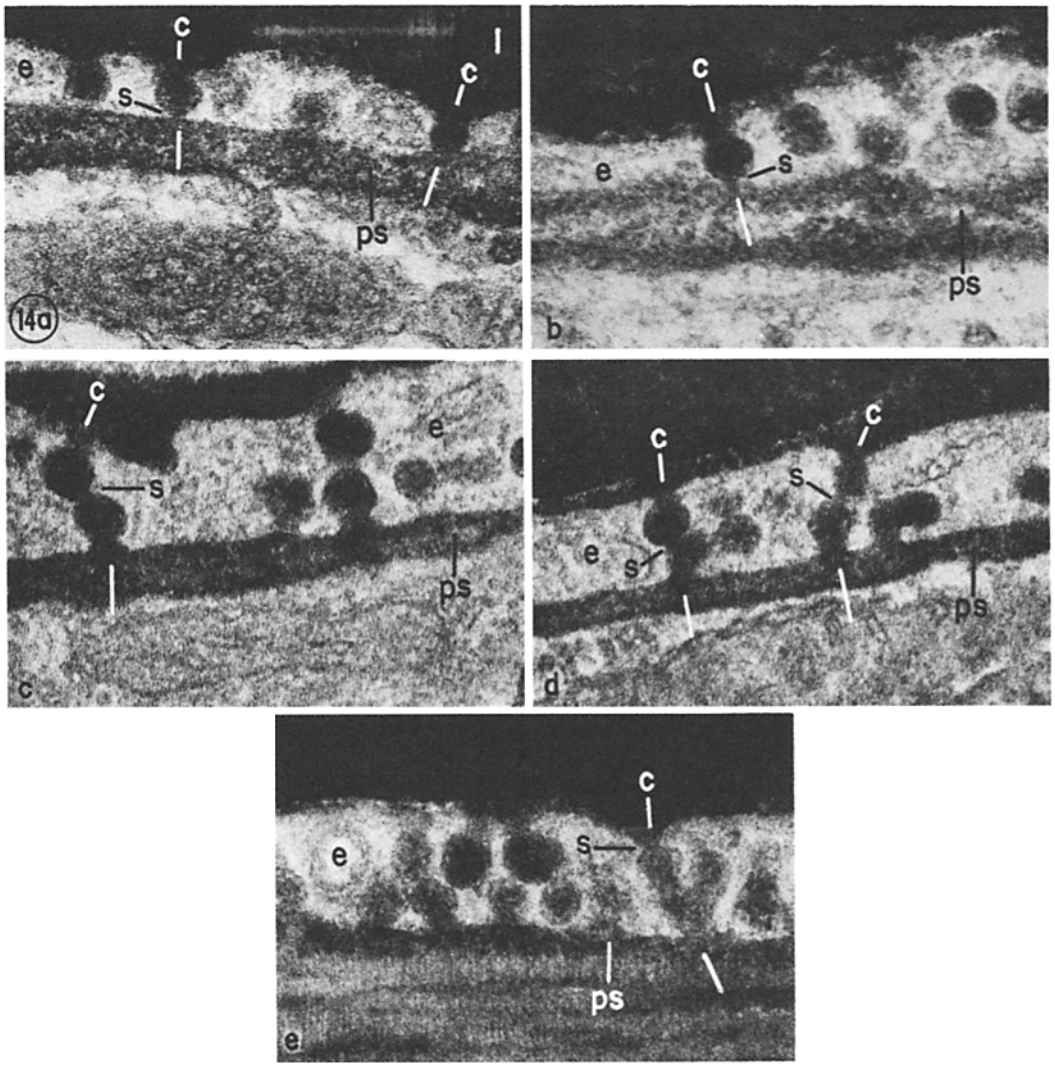

FIGURE 14 *a–e* Rat Diaphragm. Blood capillaries 1–2 min after H8P i.v. administration. One vesicle (14 *a*, *b*) and two vesicle-channels (14 *c*, *d*, *e*) as well as more complex branched structure (14 *e*) are illustrated in this series of micrographs. Note the clear examples of strictures along the channels (14 *c*, *d*) and at the openings on the blood front (14 *e*) or tissue front (14 *a*, *b*). × 68,000.

weight). By osmometry, we detected a slight increase of ~1.2% over the time interval (15–45 s) relevant for our observations, although a slight decrease of about 1.5–2% was expected, as shown by determinations carried out in vitro. The reason for this finding is unknown. We assume that the slight increase found in plasma osmolality can not radically affect plasma-tissue exchanges at the level of blood capillaries.

STATE OF HP IN THE PLASMA: In our experimental conditions, the HPs were found to occur essentially (H8P) or predominantly (H11P) in monomeric form in both tracer solutions and blood plasma. In other conditions, especially at pH 11–12, partial aggregation or polymerization has been recorded (16, 20, 31). Our evidence is based on gel filtration, a method extensively used for studying the binding of a variety of molecules (including heme-proteins) to plasma proteins. (44–47). A basic assumption in this study is that the ionic conditions in the chromatographic bed do not affect the stability of plasma proteins-HP bonds, if extant.

CROSS-LINKAGE OF HP TO PLASMA PROTEINS BY ALDEHYDE FIXATION: The experiments in Figs. 3 and 4 show that ~100% of

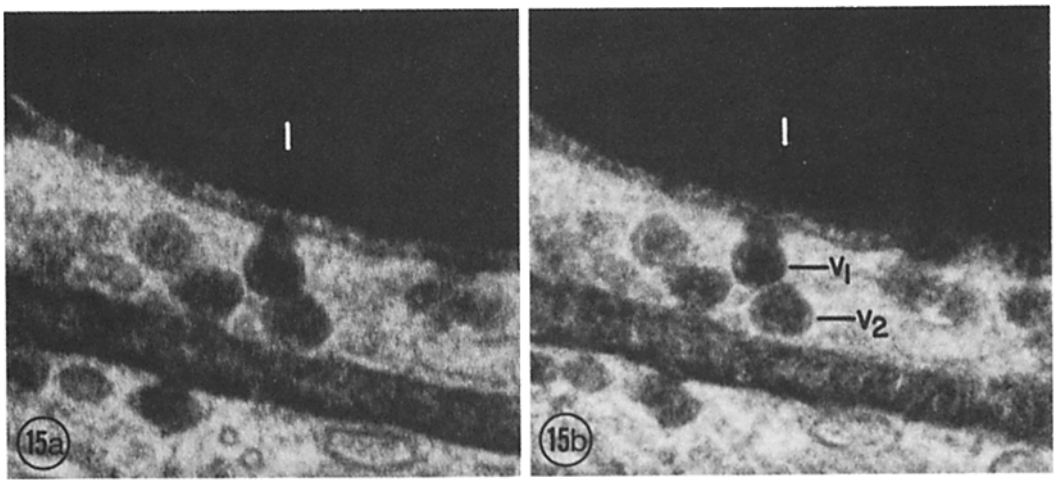

FIGURE 15 *a,b* The apparent channel in Fig. 15 *a* is resolved by a 23° tilt into a vesicle (V_1) opened on the blood front and another vesicle (V_2) isolated from the first by a space of ~50–70 Å and from the plasmalemma on the tissue front by an interval of ~100–150 Å. Preparation of the specimen as in Fig. 16. × 102,000.

added H11P is cross-linked to plasma proteins by aldehydes (3% glutaraldehyde + 5% formaldehyde) in 2 h. The corresponding value for H8P is ~50%. The difference between the two peptides is probably explained by the existence of an additional–NH_2 group (lysine) in H11P. On the basis of these results we could expect satisfactory retention of H11P in the tissue. We do not have direct data concerning loss of H8P from our specimens during tissue processing; hence, we do not know whether the efficiency of cross-linkage to tissue protein is comparable to or higher than that mentioned above. We assume that the losses are minimal since there is no difference in the intensity of the peroxidatic reaction between H11P and H8P specimens; and we believe that there is no change in H8P location in the tissue during or after fixation, since the results obtained with the two HPs are essentially identical.

Taking into account these results and those of control experiments (which show that there are no other significant sources of peroxidatic activity in the plasma), we assume that our findings reflect the interactions of individual HP molecules with the capillary wall. We consider that our experimental conditions are controlled well enough so that these interactions are not affected by excessive tracer concentration (cf. 48), and by large increases in blood volume (cf. 49), hydrostatic pressure (cf. 50), or osmolality (cf. 51).

Passageway of HPs across the Capillary Wall

GENERAL: Our findings will be discussed in terms of passage of HP molecules across the capillary wall, although it is understood that what we are detecting is a multistep RP of the injected tracers. It is assumed that, within the limits of sensitivity of our techniques, the location of the RP coincides with that of the tracer.

PLASMALEMMAL VESICLES: As in the Mb experiments (13), the only endothelial compartment marked by RP was the plasmalemmal vesicles. All other structures were free of detactable probe. This indicated that molecules in the range of ~2,000–1,500 mol wt cross the endothelium preferentially, if not exclusively, via plasmalemmal vesicles or related structures, not through intercellular junctions. By comparison with Mb, the "transit time" (52–57) of HP molecules was faster. Over the same time interval (30 s) "phase I" of the HP passage corresponded to phases I and II of the Mb experiments (13). The time lapse for the appearance of HPs in the pericapillary spaces was 45 s as opposed to 60 s for Mb. During all periods considered, the percentage of marked vesicles was higher in HP than in Mb experiments, indicating that almost the entire vesicle population of the endothelium took part in the transport of these probe molecules.

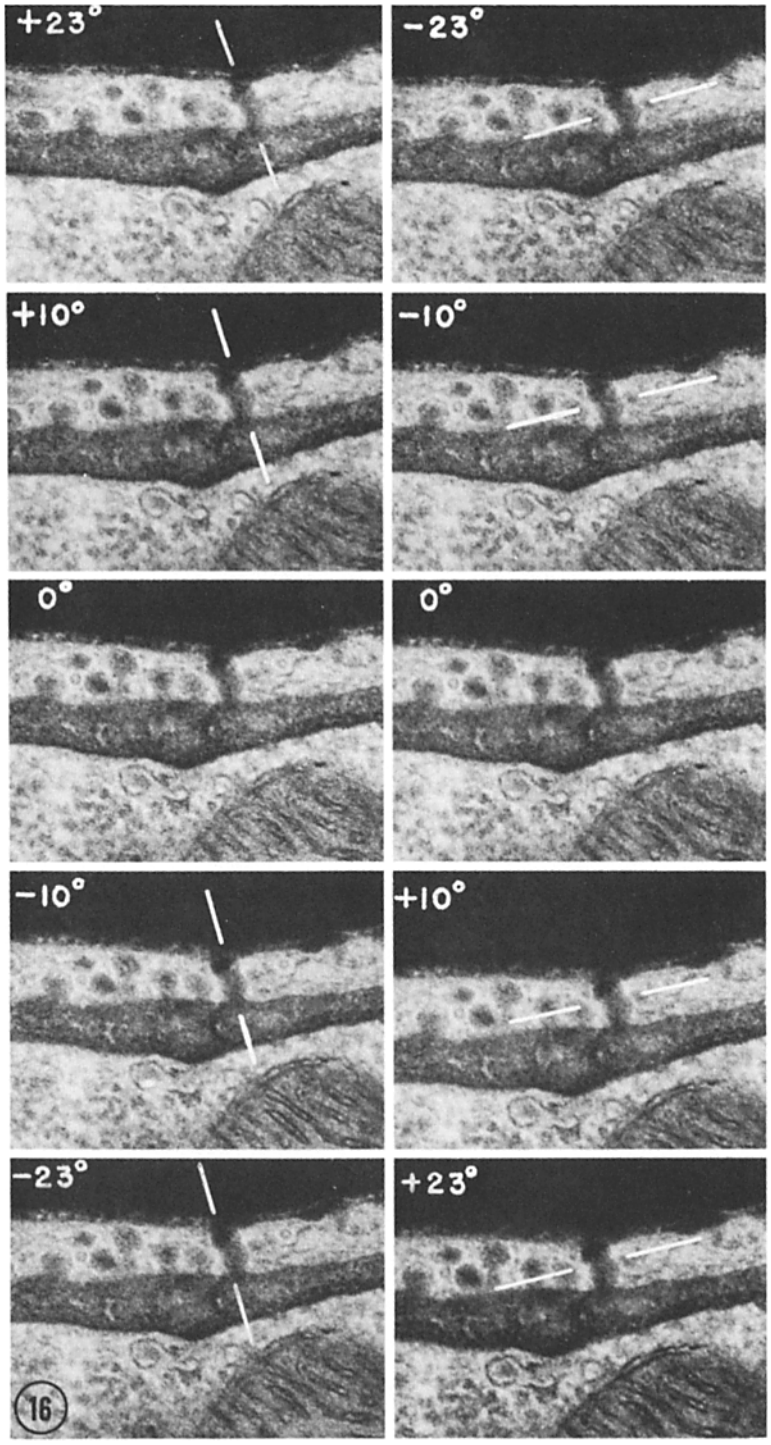

FIGURE 16 Rat diaphragm. Blood capillary 60 s after H8P injection. Analysis of a transendothelial, two vesicle-channel by specimen tilting over a range of +23° to −23° in two perpendicular directions indicated by the white lines. The channel retained its continuity in all positions. × 20,000.

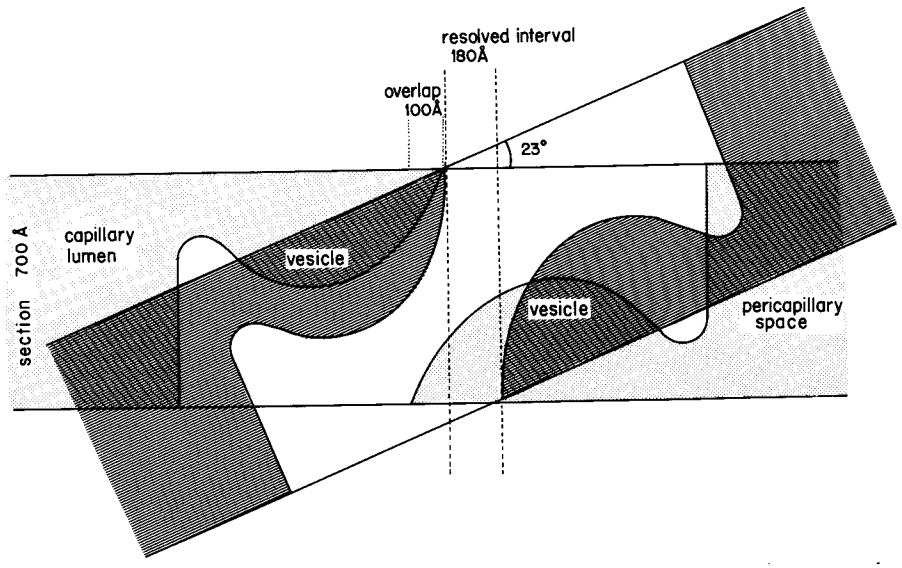

FIGURE 17 Graphic analysis of a channel image identical to that seen in Fig. 16, but assumed to be produced by two overlapping, unconnected vesicles. In this case, in a section ~700 Å thick, a tilt through a 23° angle is sufficient to resolve an overlap of 100 Å by revealing a clear space 180 Å wide between the two superimposed but unconnected vesicles. The dimensions of the structures in the graph reproduce at a higher scale the dimensions of the channel and its surroundings in Fig. 16. Actually the image in Fig. 16 was not resolved in two separate vesicles by tilting the specimen through the same angle; accordingly, it can be concluded that the image represents a true channel.

TRANSENDOTHELIAL CHANNELS: Although the existence of such channels was previously postulated (58), and occasionally claimed in some capillary profiles (59–61), their presence and structural identity have not been convincingly established. In our Mb experiments, we considered that plasmalemmal vesicles could function as small pores, provided they incatenate as continuous transendothelial channels fitted with strictures of ~90-Å diameter (13). In the HPs experiments now reported, we have detected such vesicle-derived channels with relatively high frequency. Tilting of the specimens and graphic analysis of the corresponding micrographs has shown that a sizable fraction of these images represents true channels. The rest corresponds to vesicle images superimposed in the depth of the sections. The demonstration of such channels is facilitated by a procedure[3] which increases membrane contrast and thereby allows clear visualization of continuity between plasmalemma and vesicle membranes. Channel images were also encountered in our Mb experiments, but they were not reported since they were not checked by specimen tilting and graphic analysis of micrographs to rule out overlap of isolated vesicles. We have the impression that channel images are more frequent in our HP experiments, and we believe that the difference can be attributed to the smaller dimensions of these probes.

The channels are provided with one or more strictures of ~100-Å (range 80–150 Å) diameter at the points of fusion of the incatenated vesicles and sometimes at the level of the vesicular stomata. Some of these stomata are provided with diaphragms which may have in their own structure the porosity required for the small pores as seems to be the case for the fenestral diaphragms in visceral capillaries (62).

The polymorphism of these channels (number of fused vesicles, and tridimensional geometry, including form and precise size of strictures) suggests that they are formed by random collision and fusion of vesicles and hence do not represent permanent structures of stable morphology. We have recently found that a large percentage of plasmalemmal vesicles appear to be open at any time on each front of the endothelium (63). This situation may facilitate the formation of channels by interaction of two such vesicles each located on an opposite cell front, or by the intercalation of a third vesicle coming from the interior of the cell. The polymorphism of the channels and their strictures suggests that there is no strict uniformity in the system. This is not in perfect agreement with

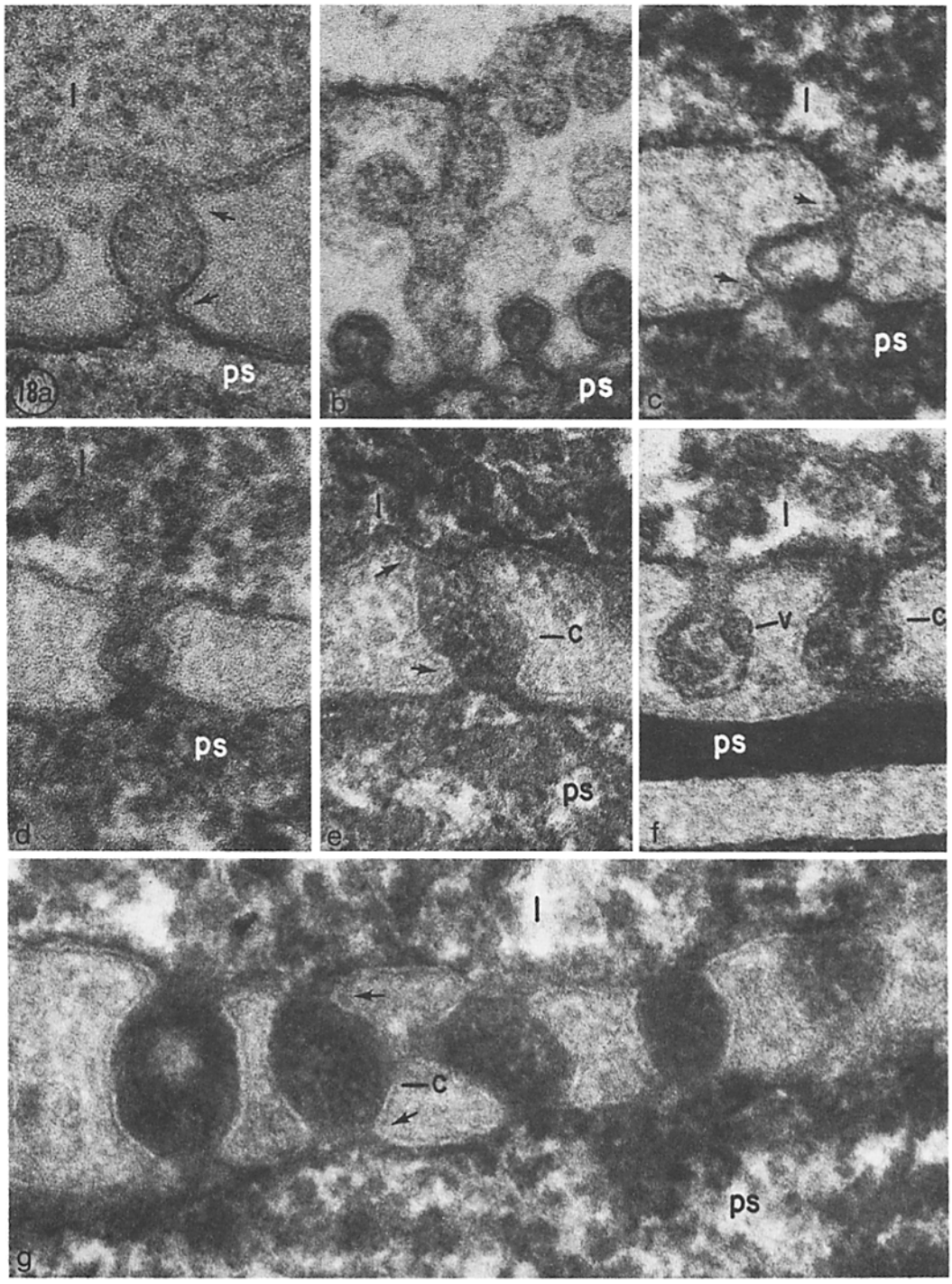

FIGURE 18 *a–g* Blood capillaries of rat diaphragm: *a*, *b*, control animals; *c*, *d*, *e*, 1 min after H11P i.v. injection; *f*, *g*, blood capillaries of rat cremaster 5 min after local interstitial injection of H11P. All specimens were treated in block with digallic acid before dehydration. RP marks the capillary lumen (*l*), the pericapillary spaces (*ps*), plasmalemmal vesicles (*v*) of usual appearance, and transendothelial channels (*c*) formed by a single vesicle in *a*, *c*, *d*, *f*, *g*, probably two vesicles in *e* and a chain of four vesicles in *b*. A high frequency of channels as in *g* was only occasionally encountered. Note that the plasmalemma and the vesicle membranes are in continuity on both sides of the channels. Overlap can be ruled out (in favor of a true channel) when membrane continuity is clearly demonstrated along one side of the channel and at one intersection point at least (out of two) at the level of each opening. Such examples are indicated by arrows. *a*, *c*, *e*, *f*, *g*, × 200,000; *b*, *d*, × 150,000.

the pore theory which basically postulates pore uniformity (4). It is, however, in agreement with a number of theoretical considerations (64, 65) and findings (66) which point to possible deviations from pore uniformity.

The channels satisfy two of the basic requirements of the pore theory: (*a*) they are water-filled passages connecting across the endothelium the capillary lumen with the tissue spaces; (*b*) they are provided with size limiting structures of ~100 Å (range 80–150 Å). Their definitive identification as structural equivalent of the small pores depends on their frequency per unit of endothelial surface. Our impression is that they are reasonably frequent[7], but precise frequency figures remain to be established by future work.

INTERCELLULAR JUNCTIONS: Within the limits of sensitivity of the cytochemical techniques used, and within the time intervals over which initial transport from the plasma to the tissue spaces can be detected (0–40 s), the large majority of the intercellular junctions of the endothelium appears free of RP. The intercellular spaces beyond the junctions begin to be RP marked only in phase III (40–60 s) in concentrations which suggest back diffusion from the pericapillary spaces, rather than the reverse. The finding that HP molecules do not pass through the endothelial junctions in detectable amounts does not rule out the possible diffusion of smaller molecules along these intercellular pathways. Recent physiological data indicate that in some epithelia (67–73) and mesothelia (74–75), diffusion of water, ions, and small molecules occurs along the intercellular spaces through "leaky" tight junctions. Attempts have been made to correlate the degree of leakiness with the degree of structural organization of the occluding zonules, and the hypothesis advanced is that the tightness increases with the number of ridges positioned in series in an occluding zonule (76). The relevant information is obtained on replicas in freeze-cleaved specimens.

As reported in reference 77, simplified tight junctions can be demonstrated in the endothelium of muscle and visceral capillaries on freeze-cleaved specimens. These junctions resemble in part those found in the proximal convoluted tubules of the nephron, and by analogy they are expected to be permeable to water and small molecules of the size of sucrose (~10 Å) or larger. Complete data are not available so that the size limit for diffusion through leaky junctions remains to be established in the nephron as well as in the endothelium.

Under the conditions of our experiments it appears that molecules of ~20 Å (diameter of our HP tracers) do not cross the endothelium along the tight junctions, but via vesicles either isolated or organized in patent channels. These channels appear, therefore, as the most likely candidates for structural equivalents of the small pore system (postulated pore diameter: 50–90 Å). We recognize, however, that we can not rule out perturbations introduced by our experimental approach in forces operating at the level of the capillary walls. But, larger variations in osmolality, blood volume, and hydrostatic pressure can be introduced in future experiments to find out within what limits our conclusions hold.

We gratefully acknowledge the excellent technical assistance of Heide Plesken, Pam Stenard, and John Albert.

Parts of these results were presented at the XIII Annual Meeting of The American Society for Cell Biology, Miami Beach, Florida, 1973, and appeared as an abstract in *J. Cell Biol.* 1973. **59**(2, Pt. 2):318 a.

Received for publication 15 March 1974, and in revised form 15 October 1974.

REFERENCES

1. PAPPENHEIMER, J. R., E. M. RENKIN, and L. M. BORRERO. 1951. Filtration, diffusion and molecular sieving through peripheral capillary membranes. A contribution to the pore theory of capillary permeability. *Am. J. Physiol.* **167**:13.
2. PAPPENHEIMER, J. R. 1953. Passage of molecules through capillary walls. *Physiol. Rev.* **33**:387.
3. GROTTE, G. 1956. Passage of dextran molecules across the blood-lymph barrier. *Acta Chir. Scand.* **211**(Suppl.):1.
4. LANDIS, E. M., and J. R. PAPPENHEIMER. 1963. Exchange of substance through the capillary walls. *In* Handbook of Physiology. W. F. Hamilton and P. Dow, editors. American Physiology Society, Washington D.C. **2**(2):961.
5. LASSEN, N. A., and J. TRAP-JENSEN. 1970. Estimation of the fraction of the inter-endothelial slit which must be open in order to account for the observed transcapillary exchange of small hydrophilic mole-

[7] We should point out that in a tridimensional reconstruction of a small segment of the endothelium of a blood capillary (rat diaphragm), short chains of interconnected vesicles were found, but patent channels were not detected (58). The apparent discrepancy with the findings now reported can be explained by the small volume of the reconstructed sample.

cules in skeletal muscle in man. *In* Capillary Permeability. Alfred Benzon Symposium II. Ch. Crone, and N. A. Lassen, editors. Academic Press, Inc., New York. 647.

6. MAEHLY, A. C. 1955. Plant Peroxidase. *In* Methods in Enzymology. Colowick, S. P. and Kaplan, N. O., editors. Academic Press, Inc., New York. **2**:807.
7. MARGOLIASH, E., N. FROHWIRT, and E. WEINER. 1959. A study of the cytochrome *c* haemochromogen. *Biochem. J.* **71**:559.
8. DICKERSON, R. E., T. TAKANO, D. EISENBERG, O. B. KALLAI, L. SAMSON, A. COOPER, and E. MARGOLIASH. 1971. Ferricytochrome *c*. General features of the horse and bonito proteins at 2.8 A resolution. *J. Biol. Chem.* **246**:1511.
9. KARNOVSKY, M. J. 1967. The ultrastructural basis of capillary permeability studied with peroxidase as a tracer. *J. Cell Biol.* **35**:213.
10. KARNOVSKY, M. J., and D. F. RICE. 1969. Exogenous cytochrome *c* as an ultrastructural tracer. *J. Histochem. Cytochem.* **17**:751.
11. KARNOVSKY, M. J. 1970. Morphology of capillaries with special reference to muscle capillaries. *In* Capillary Permeability. Alfred Benzon Symposium II. Ch. Crone and N. A. Lassen, editors. Academic Press, Inc., New York. 341.
12. KENDREW, J. C., G. BODO, H. M. DINTZIS, R. G. PARRISH, H. WYCKOFF, and D. C. PHILLIPS. 1958. A three-dimensional model of the myoglobin molecule obtained by X-ray analysis. *Nature (Lond.).* **181**:662.
13. SIMIONESCU, N., M. SIMIONESCU, and G. E. PALADE. 1973. Permeability of muscle capillaries to exogenous myoglobin. *J. Cell Biol.* **57**:424.
14. FEDER, N., T. S. REESE, and M. W. BRIGHTMAN. 1969. Microperoxidase, a new tracer of low molecular weight. A study of the interstitial compartments of the mouse brain. *J. Cell Biol.* **43**(2, Pt. 2):35 a. (Abstr.).
15. FEDER, N. 1970. A heme-peptide as an ultrastructural tracer. *J. Histochem. Cytochem.* **18**:911.
16. FEDER, N. 1971. Microperoxidase. An ultrastructural tracer of low molecular weight. *J. Cell Biol.* **51**:339.
17. BRIGHTMAN, M. W., T. S. REESE, and N. FEDER. 1970. Assessment with the electron microscope of the permeability to peroxidase of cerebral endothelium and epithelium in mice and sharks. *In* Capillary Permeability. Alfred Benzon Symposium II. Ch. Crone and N. A. Lassen, editors. Academic Press, Inc., New York. 463.
18. TSOU, C. L. 1951. Cytochrome *c* modified by digestion with proteolytic enzymes. I. Digestion. *Biochem. J.* **49**:362.
19. TUPPY, H., and S. PALÉUS. 1955. Study of a peptic degradation product of cytochrome *c*. I. Purification and chemical composition. *Acta Chem. Scand.* **9**:353.
20. HARBURY, H. A., and P. A. LOACH. 1960. Oxidation linked proton functions in heme octa- and undecapeptides from mammalian cytochrome *c*. *J. Biol. Chem.* **235**:3640.
21. KRAEHENBUHL, J. P., R. E. GALARDY, and J. D. JAMIESON. 1974. Preparation and characterization of an immunoelectron microscope tracer consisting of a heme-octapeptide coupled to FAB. *J. Exp. Med.* **139**:208.
22. GOTH, A., and M. KNOOHUIZEN. 1966. Genetically conditioned dextran co-factor in the rat. *Fed. Proc.* **25**:692.
23. COTRAN, R., and M. J. KARNOVSKY. 1968. Resistance of Wistar-Furth rats to the mast cell-damaging effect of horseradish peroxidase. *J. Histochem. Cytochem.* **16**:382.
24. SIMIONESCU, N., and G. E. PALADE. 1971. Dextrans and glycogens as particulate tracers for studying capillary permeability. *J. Cell Biol.* **50**:616.
25. MAJNO, G., and G. E. PALADE. 1961. Studies on inflammation. I. The effect of histamine and serotonin on vascular permeability; an electron microscopic study. *J. Biophys. Biochem. Cytol.* **11**:571.
26. GRAHAM, R. C., and M. J. KARNOVSKY. 1966. The early stage of absorption of injected horseradish peroxidase in the proximal tubule of the mouse kidney. Ultrastructural cytochemistry by a new technique. *J. Histochem. Cytochem.* **14**:291.
27. TU, A. T., J. A. REINOSA, and Y. Y. HSIAO. 1968. Peroxidative activity of hemepeptides from horse heart cytochrome *c*. *Experientia (Basel).* **24**:219.
28. PALÉUS, S., A. EHRENBERG, and H. TUPPY. 1955. Study of a peptic degradation product of cytochrome *c*. II. Investigation of the linkage between peptide moiety and prosthetic group. *Acta Chem. Scand.* **9**:365.
29. EHRENBERG, A., and H. THEORELL. 1955. On the stereo-chemical structure of cytochrome *c*. *Acta Chem. Scand.* **9**:1193.
30. HARBURY, H. A., and P. A. LOACH. 1959. Linked functions in heme systems; oxidation-reduction potentials and adsorption spectra of a heme-peptide obtained upon peptic hydrolysis of cytochrome *c*. *Proc. Natl. Acad. Sci. U. S. A.* **45**:1344.
31. HOARD, J. L. 1971. Stereochemistry of hemes and other metalloporphyrins. *Science (Wash. D. C.).* **174**:1295.
32. DICKERSON, R. E. 1972. The structure and history of an ancient protein. *Sci. Am.* **226**:58.
33. WIENFIELD, M. E. 1965. Electron transfer within and between hemoprotein molecules. *J. Mol. Biol.* **12**:600.
34. MARGOLIASH, E., W. M. FITCH, and R. E. DICKERSON. 1971. Molecular expression of evolutionary phenomena in the primary and tertiary structures of cytochrome *c*. *In* Biochemical Evolution and the Origin of Life. E. Schoffeniels, editor. North Holland Publishing Co., Amsterdam. 52.

35. CASTRO, C. E. 1971. Theory of hemeprotein reactivity. *J. Theor. Biol.* **33**:475.
36. KAMINSKY, L. S., V. J. MILLER, and A. J. DAVISON. 1973. Thermodynamic studies of the opening of the heme crevice of ferricytochrome *c*. *Biochemistry*. **12**:2215.
37. HARBURY, H. A., and P. A. LOACH. 1960. Interaction of nitrogenous ligands with heme-peptides from mammalian cytochrome *c*. *J. Biol. Chem.* **235**:3646.
38. SCHEJITER, A., and J. AVIRAM. 1969. The reaction of cytochrome *c* with imidazole. *Biochemistry*. **8**:149.
39. MYER, Y. P., and H. A. HARBURY. 1966. Optical rotatory dispersion of cytochrome *c*. II. Comparative data for a heme-octapeptide. *J. Biol. Chem.* **241**:4299.
40. HARBURY, H. A., J. R. CRONIN, M. W. FAUGER, T. P. HETTINGER, A. J. MURPHY, Y. P. MYER, and S. N. VINOGRADOV. 1965. Complex formation between methionine and a heme peptide from cytochrome *c*. *Proc. Natl. Acad. Sci. U. S. A.* **54**:1658.
41. MARGOLIASH, E., S. FERGUSON-MILLER, J. TULLOSS, C. H. KANG, B. A. FEINBERG, D. L. BRAUTIGAN, and M. MORRISON. 1973. Separate intramolecular pathways for reduction and oxidation of cytochrome *c* in electron transport chain reactions. *Proc. Natl. Acad. Sci. U. S. A.* **70**:3245.
42. BABUL, G., and E. STELLWAGEN. 1971. The existence of heme-protein coordinate-covalent bonds in denaturating solvents. *Biopolymers*. **10**:2359.
43. SUTIN, N., and J. K. YANDELL. 1972. Mechanisms of the reactions of cytochrome *c*. Rate and equilibrium constants for ligand bindings to horse heart ferricytochrome *c*. *J. Biol. Chem.* **247**:6932.
44. KILLANDER, J. 1964. Separation of human heme- and hemoglobin-binding plasma proteins, ceruloplasmin and albumin by gel filtration. *Biochem. Biophys. Acta*. **93**:1.
45. COOPER, P. F., and G. C. WOOD. 1968. Protein-binding of small molecules: new gel filtration method. *J. Pharm. Pharmacol.* **20**(Suppl.):150S.
46. WOOD, G. C., and P. F. COOPER. 1970. The application of gel filtration to the study of protein-binding of small molecules. *Chromatogr. Rev.* **12**:88.
47. VEGGE, T., F. Ø. WINTHER, and B. R. OLSEN. 1971. Horseradish peroxidase in plasma studied by gel filtration. *Histochemie*. **28**:16.
48. CLEMENTI, F. 1970. Effect of horseradish peroxidase on mice lung capillaries permeability. *J. Histochem. Cytochem*. **18**:226.
49. SCHNEEBERGER, E. E., and M. J. KARNOVSKY. 1971. The influence of intravascular fluid volume on the permeability of newborn and adult mouse lungs to ultrastructural protein tracers. *J. Cell Biol.* **49**:319.
50. HÜTTNER, I., M. BOUTET, and R. H. MORE. 1971. The effect of pressure on the passage of fine structural proteins through arterial endothelium. Eleventh Annual Meeting of The American Society for Cell Biology, New Orleans. 134. (Abstr.).
51. WADE, J. B., and V. A. DISCALA. 1971. The effect of osmotic flow on the distribution of horseradish peroxidase within the intercellular spaces of toad bladder epithelium. *J. Cell Biol.* **51**:553.
52. BRUNS, R. R., and G. E. PALADE. 1968. Studies on blood capillaries. II. Transport of ferritin molecules across the wall of muscle capillaries. *J. Cell Biol.* **37**:277.
53. RENKIN, E. M. 1964. Transport of large molecules across capillary walls. *Physiologist*. **7**:13.
54. SHEA, ST. M., and M. J. KARNOVSKY. 1969. Vesicular transport across endothelium: simulation of a diffusion model. *J. Theor. Biol.* **24**:30.
55. TOMLLIN, S. G. 1969. Vesicular transport across endothelial cells. *Biochim. Biophys. Acta*. **13**:559.
56. GREEN, H. S., and J. R. CASLEY-SMITH. 1972. Calculations on the passage of small vesicles across endothelial cells by brownian motion. *J. Theor. Biol.* **35**:103.
57. SHEA, ST. M., and W. H. BOSSERT. 1973. Vesicular transport across endothelium: a generalized diffusion model. *Microvasc. Res.* **6**:305.
58. BRUNS, R. R., and G. E. PALADE. 1968. Studies on blood capillaries. I. General organization of blood capillaries in muscle. *J. Cell Biol.* **37**:244.
59. KOBAYASHI, S. 1970. Occurrence of unique colloidal particles in snake blood and their transport across the capillary wall. A proposal of a new hypothesis on the permeability of the blood capillaries. *Arch. Histol. Jap.* **31**:511.
60. HASHIMOTO, P. 1972. Intercellular channels as a route for protein passage in the capillary endothelium of the shark brain. *Am. J. Anat.* **134**:41.
61. ZWEIFACH, B. W. 1972. Capillary filtration and mechanisms of edema formation. *Pflügers Arch. Eur. J. Physiol.* **336**(Suppl.):81S.
62. CLEMENTI, F., and G. E. PALADE. 1969. Intestinal capillaries. I. Permeability to peroxidase and ferritin. *J. Cell Biol.* **41**:33.
63. SIMIONESCU, M., N. SIMIONESCU, and G. E. PALADE. 1974. Morphometric data on the endothelium of blood capillaries. *J. Cell Biol.* **60**:128.
64. MALONE, G. H., S. PRAGER, and T. E. HUTCHINSON. 1972. A simple model for diffusion in independent, temporally fluctuating pores. *J. Theor. Biol.* **36**:379.
65. PATLAK, C. S., and S. I. RAPOPORT. 1971. Theoretical analysis of net tracer flux due to volume circulation in a membrane with pores of different sizes. Relation to solute drag model. *J. Gen. Physiol.* **57**:113.
66. DIANA, J. N., S. C. LONG, and H. YAO. 1972. Effect of histamine on equivalent pore radius in capillaries of isolated dog hindlimb. *Microvasc. Res.* **4**:413.
67. TORMEY, J. MCD., and J. M. DIAMOND. 1967. The ultrastructural route of fluid transport in rabbit gall bladder. *J. Gen. Physiol.* **50**:2031.
68. SMULDERS, A. P., J. MCD. TORMEY, and E. M. WRIGHT. 1972. The effect of osmotically induced

water flows on the permeability and ultrastructure of the rabbit gall bladder. *J. Membr. Biol.* **7**:164.

69. WRIGHT, E. M., A. P. SMULDERS, and J. MCD. TORMEY. 1972. The role of the lateral intercellular spaces and solute polarization effects in the passive flow of water across the rabbit gall bladder. *J. Membr. Biol.* **7**:198.
70. FRÖMTER, E. 1972. The route of passive ion movement through the epithelium of Necturus gall bladder. *J. Membr. Biol.* **8**:259.
71. DIBONA, D. R. 1972. Passive intercellular pathway in amphibian epithelia. *Nat. New Biol.* **238**:179.
72. DIAMOND, J., and E. FRÖMTER. 1972. Route of passive ion permeation in epithelia. *Nature (Lond.).* **235**:9.
73. WADE, J. B., J. P. REVEL, and V. A. DISCALA. 1973. Effect of osmotic gradients on intercellular junctions of the toad bladder. *Am. J. Physiol.* **224**:407.
74. GOSSELIN, R. E., and W. O. BERNDT. 1962. Diffusional transport of solutes through mesentery and peritoneum. *J. Theor. Biol.* **3**:487.
75. MICHEL, C. C. 1970. Direct observations of sites of permeability for ions and small molecules in mesothelium and endothelium. *In* Capillary Permeability. Alfred Benzon Symposium II. Ch. Crone and N. A. Lassen, editors. Academic Press, Inc., New York. 647.
76. CLAUDE, PH., and D. A. GOODENOUGH. 1973. Fracture faces of zonulae occludentes from "tight" and "leaky" epithelia. *J. Cell Biol.* **58**:390.
77. SIMIONESCU, M., N. SIMIONESCU, and G. E. PALADE. 1974. Characteristic endothelial junctions in sequencial segments of the microvasculature. Abstracts from the Fourteenth Annual Meeting of The American Society for Cell Biology, San Diego, California. *J. Cell Biol.* **63**(2, Pt. 2):316 a. (Abstr.).